A comparison of the transport properties of bilayer graphene, monolayer graphene, and two-dimensional electron gas*

Sun Li-Feng(孙立凤)[a], Dong Li-Min(董利民)[b], Wu Zhi-Fang(吴志芳)[a], and Fang Chao(房 超)[a]†

[a] *Institute of Nuclear and New Energy Technology, Tsinghua University, Beijing* 100084, *China*

[b] *Beijing Key Laboratory of Fine Ceramics, Institute of Nuclear and New Energy Technology, Tsinghua University, Beijing* 100084, *China*

(Received 22 January 2013; revised manuscript received 25 February 2013)

We studied and compared the transport properties of charge carriers in bilayer graphene, monolayer graphene, and the conventional semiconductors (the two-dimensional electron gas (2DEG)). It is elucidated that the normal incidence transmission in the bilayer graphene is identical to that in the 2DEG but totally different from that in the monolayer graphene. However, resonant peaks appear in the non-normal incidence transmission profile for a high barrier in the bilayer graphene, which do not occur in the 2DEG. Furthermore, there are tunneling and forbidden regions in the transmission spectrum for each material, and the division of the two regions has been given in the work. The tunneling region covers a wide range of the incident energy for the two graphene systems, but only exists under specific conditions for the 2DEG. The counterparts of the transmission in the conductance profile are also given for the three materials, which may be used as high-performance devices based on the bilayer graphene.

Keywords: bilayer graphene, monolayer graphene, two-dimensional electron gas (2DEG), transport properties

PACS: 72.80.Vp, 73.23.Ad, 73.40.Gk **DOI:** 10.1088/1674-1056/22/7/077201

1. Introduction

A large amount of interest has been aroused in the research on the physical properties of graphene[1,2] since the graphitic sheet of one-atom thickness was experimentally realized by Novoselov *et al.*[3] The reason is that the electronic properties of graphenes, including the monolayer, bilayer, and multilayer graphenes, are drastically different from the conventional semiconductors. Charge carriers in the monolayer graphene behave like relativistic chiral massless particles with a "light speed" equal to the Fermi velocity and possess a gapless linear spectrum at low energy.[3–5] As a result, the monolayer graphene exhibits a number of unique electronic and transport properties, such as Klein tunneling,[6] the unconventional quantum Hall effect,[4,7–10] a strong electric effect,[11] finite minimal conductivity,[7,12–15] and the special Andreev reflection.[16,17]

There are some basic similarities and differences between the bilayer graphene and the monolayer graphene. On one hand, the charge carriers in the bilayer graphene are chiral and described by spinor wavefunctions, similar to the relativistic particles or quasiparticles in the monolayer graphene.[6,18] On the other hand, in contrast to the charge carriers in the monolayer graphene, those in the bilayer graphene possess a parabolic spectrum at low energy, which means that they are massive Dirac fermions[9,19] with a finite density of states at zero energy, similar to the conventional unrelativistic electrons. There have been many studies on the bilayer graphene about the quantum Hall effects,[12] bandgap engineering,[9,19–23] transmission,[24,25] transportation related with the Berry phase,[12,26,27] and collimation.[6] However, more studies on the transport properties of the bilayer graphene may be necessary to understand the massive Dirac fermions. Some researchers have studied the resonant tunneling of the electrons in the bilayer graphene, but most of them focused on the transmission for the normal incidence or for a very high barrier ($V > 2E$).[6,18,28] As we know, there is a transmission gap (as a function of the incident energy) when the electrons incident obliquely and the energy approaches to the height of the potential barrier ($E \approx V$).[29,30] The conductance at the Dirac point for a monolayer graphene nanoribbon is independent of contacts with dense modes.[31] Then, what about the transport properties in the bilayer graphene in this case? Can the massive Dirac fermions exhibit any new features different from the massless Dirac fermions and the conventional unrelativistic electrons?

To study these questions, we consider the transport properties of the massive Dirac fermions for an arbitrary incident angle and wide-range incident energy covering from the high barrier case ($E < V$) to the low barrier case ($E > V$). The transmission and conductance for the bilayer graphene, the monolayer graphene, and the conventional semiconductors (here we take the two-dimensional electron gas as an example) have been calculated and compared. It is found that the trans-

*Project supported by the National Natural Science Foundation of China (Grant No. 11104156), the Postdoctoral Science Foundation of China (Grant No. 2012M510405), the Independent Research and Development Fund of Tsinghua University, China (Grant No. 20121087948), and the Beijing Key Lab of Fine Ceramics Opening Fund, China (Grant No. 2012200110).

†Corresponding author. E-mail: fangchao@mail.tsinghua.edu.cn

© 2013 Chinese Physical Society and IOP Publishing Ltd

port properties of the electrons in the bilayer graphene display some similarities but also dramatic differences with those in the other two materials.

2. Model and method

We consider the massive quasiparticles in the bilayer graphene incidenting upon a two-dimensional (2D) potential barrier with incident energy E at angle ϕ, then they are formally described by an off-diagonal Hamiltonian[9,12]

$$\boldsymbol{H} = -\frac{\hbar^2}{2m_{\rm e}}\begin{pmatrix} 0 & (k_x - {\rm i}k_y)^2 \\ (k_x + {\rm i}k_y)^2 & 0 \end{pmatrix} + V(x), \qquad (1)$$

where $V(x)$ equals U_0 inside the barrier and zero elsewhere. Since the y component of the electron momentum operator commutes with the Hamiltonian, the spinor wavefunction can be written as $\Psi(x,y) = \begin{pmatrix} \psi_{\rm I}(x) & \psi_{\rm II}(x) \end{pmatrix}^{\rm T} {\rm e}^{{\rm i}k_y y}$. To simplify the notation, we express all the quantities in dimensionless units: $x \to x/D_0$, $E \to EE_{\rm b0}$, $V \to VE_{\rm b0}$, and $E_{\rm b0} = \hbar^2/\left(2m_{\rm e}D_0^2\right)$. For $D_0 = 10$ nm, $E_{\rm b0} \approx 0.038$ meV.

There are drastic differences between the bilayer graphene, the monolayer graphene, and the two-dimensional electron gas (2DEG), though the charge carriers in the three materials are all restricted in a 2D plane. The electrons and holes in the 2DEG are normally described by separate Schrödinger equations, which are not connected in any way. In contrast, the electrons and holes in the two graphene systems are interconnected, exhibiting chiral properties. They are both described by two-component wavefunctions. Furthermore, there are four possible solutions with a given energy E for the bilayer graphene, among which two correspond to propagating waves and the other two to evanescent waves. This is an important difference in the tunneling between the bilayer graphene and the other two 2D materials. The eigenstates of the Hamiltonian in Eq. (1) can be written in the following form:

$$\psi_{\rm bI} = \begin{cases} {\rm e}^{{\rm i}k_x x} + r{\rm e}^{-{\rm i}k_x x} + c_1 {\rm e}^{\alpha x}, & x < 0, \\ a_2 {\rm e}^{{\rm i}q_x x} + b_2 {\rm e}^{-{\rm i}q_x x} + c_2 {\rm e}^{\beta x} + d_2 {\rm e}^{-\beta x}, & 0 \le x \le D, \\ t{\rm e}^{{\rm i}k_x x} + d_3 {\rm e}^{-\alpha x}, & x > D, \end{cases} \qquad (2)$$

$$\psi_{\rm bII} = \begin{cases} -{\rm e}^{{\rm i}k_x x + 2{\rm i}\phi} - r{\rm e}^{-{\rm i}k_x x - 2{\rm i}\phi} + c_1 h_1 {\rm e}^{\alpha x}, & x < 0, \\ s_2\left(a_2 {\rm e}^{{\rm i}q_x x + 2{\rm i}\theta} + b_2 {\rm e}^{-{\rm i}q_x x - 2{\rm i}\theta} - c_2 h_2 {\rm e}^{\beta x} - d_2 {\rm e}^{-\beta x}/h_2\right), & 0 \le x \le D, \\ -t{\rm e}^{{\rm i}k_x x + 2{\rm i}\phi} + d_3 {\rm e}^{-\alpha x}/h_1, & x > D, \end{cases} \qquad (3)$$

where $s_2 = {\rm sgn}(U_0 - E)$, $k_x = \sqrt{E}\cos\phi$, $q_x = \sqrt{|E-U_0|}\cos\theta$, $\alpha = \sqrt{E\left(1+\sin^2\phi\right)}$, $\beta = \sqrt{|E-U_0|\left(1+\sin^2\theta\right)}$, $h_1 = \left(\sqrt{1+\sin^2\phi} - \sin\phi\right)^2$, and $h_2 = \left(\sqrt{1+\sin^2\theta} - \sin\theta\right)^2$. Coefficients r and t are the reflection and the transmission amplitudes, respectively. In terms of the conversion of the perpendicular wave vector, we can get the relationship between the angles inside and outside the potential barrier

$$\sqrt{|E-U_0|}\sin\theta = \sqrt{E}\sin\phi, \qquad (4)$$

which implies that the electrons can travel through the barrier only if $\sqrt{E/|E-U_0|}\,|\sin\phi| \le 1$. When $U_0/\left(1+\sin^2\phi\right) < E < U_0/\cos^2\phi$, θ and the wave vector q_x are then imaginary, which correspond to the evanescent propagation inside the barrier.

Matching the continuity conditions for both components of the wavefunctions and their derivatives, we can obtain the transmission coefficient by using the transfer matrix method. After obtaining the transmission coefficient, the conductance can be derived by integrating the transmission coefficient $\mathscr{T}$ over one half of the (Fermi) energy surface by using the Büttiker formula[18,28]

$$G(E) = G_0 \int_{-\pi/2}^{\pi/2} \mathscr{T}(E, \sqrt{2E}\sin\phi)\cos\phi\,{\rm d}\phi, \qquad (5)$$

where $G_0 = {\rm e}^2 m_{\rm e} v_{\rm F} l/\hbar^2$, and l is the length of the system in the y direction.

We provide the details for the other two 2D materials for comparison. As is well known, the monolayer graphene is a two-dimensional gapless semiconductor with a linear dispersion relation,[6] and its low-energy quasiparticles are formally described by the Dirac equation $[v_{\rm F}\boldsymbol{\sigma}\cdot\boldsymbol{p} + V(x)]\Psi(x,y) = E\Psi(x,y)$, where $\boldsymbol{p}$ is the momentum operator, and $v_{\rm F} \approx 10^6$ m/s is the Fermi velocity. Similar to the dimensionless method for the bilayer graphene, all the quantities can be simplified for the monolayer graphene with $x \to x/D_0$, $E \to EE_{\rm m0}$, $V \to VE_{\rm m0}$, $E_{\rm m0} = \hbar v_{\rm F}/D_0$, where D_0 is the length unit.[30] For $D_0 = 10$ nm, $E_{\rm m0} \approx 56.6$ meV. The Dirac spinor wavefunction can be expressed as

$$\psi_{\rm mI} = \begin{cases} {\rm e}^{{\rm i}k_x x} + r{\rm e}^{-{\rm i}k_x x}, & x < 0, \\ a{\rm e}^{{\rm i}q_x x} + b{\rm e}^{-{\rm i}q_x x}, & 0 \le x \le D, \\ t{\rm e}^{{\rm i}k_x x}, & x > D, \end{cases} \qquad (6)$$

$$\psi_{\rm mII} = \begin{cases} {\rm e}^{{\rm i}\phi}{\rm e}^{{\rm i}k_x x} - r{\rm e}^{-{\rm i}\phi}{\rm e}^{-{\rm i}k_x x}, & x < 0, \\ s_2\left(a{\rm e}^{{\rm i}\theta}{\rm e}^{{\rm i}q_x x} - b{\rm e}^{-{\rm i}\theta}{\rm e}^{-{\rm i}q_x x}\right), & 0 \le x \le D, \\ t{\rm e}^{{\rm i}\phi}{\rm e}^{{\rm i}k_x x}, & x > D, \end{cases} \qquad (7)$$

where $k_x = \sqrt{E^2 - k_y^2} = E\cos\phi$ and $q_x = \sqrt{(E-U_0)^2 - k_y^2} = |E-U_0|\cos\theta$ are the parallel wave vector components outside and inside the barrier, respectively. According to the conver-

sation of the perpendicular wave vector, we can obtain

$$|E-U_0|\sin\theta = E\sin\phi. \tag{8}$$

Like the analysis of the bilayer graphene, it is obvious that the electrons can travel through the barrier only if $|E/(E-U_0)\sin\phi| \leq 1$ and the evanescent modes will appear inside the barrier when $U_0/(1+\sin|\phi|) < E < U_0/(1-\sin|\phi|)$.

The electrons of the 2DEG are described by the Schrödinger equation

$$\left(P^2/(2m^*)+V(x)\right)\Psi(x,y) = E\Psi(x,y),$$

where m^* is the effective mass of an electron and can be taken as $0.067m_e$ (m_e is the free-electron mass) for GaAs. For convenience, we adopt the energy unit $E_{20} = \hbar^2/\left(2m^*D_0^2\right)$, which approximately equals 0.568 meV for $D_0 = 10$ nm. And the electrons can transport through the barrier only if $E > U_0/\cos^2\phi$. Though the energy units for the three materials are different for a unified length unit, it will not affect the comparison results about the transport properties. The aim of this work is to investigate the transportation from $E < U_0$ to $E > U_0$, which is qualitative but emphasizes on the concrete values of the incident energy and the potential barrier.

3. Numerical results and discussion

First, we consider the electrons in the bilayer graphene incidenting upon the potential barrier normally. For the low barriers ($E > U_0$), $s_2 = -1$, $\theta = \phi = 0$, then $\Psi_{\rm I} = -\Psi_{\rm II}$ both outside and inside the barrier, and the chirality of the massive Dirac fermions does not manifest itself. In this case, the transmission coefficient is

$$\mathscr{T}_{\rm b} = \left[1+\frac{\left(k_x^2-q_x^2\right)^2}{4k_x^2q_x^2}\sin^2(q_xD)\right]^{-1}, \tag{9}$$

which oscillates and reaches unity when the phase inside the barrier satisfies $q_xD = m\pi$. While for the high barriers ($E < U_0$), $s_2 = 1$, then the solutions for the bilayer graphene satisfy $\Psi_{\rm I} = -\Psi_{\rm II}$ outside the barrier and $\Psi_{\rm I} = \Psi_{\rm II}$ inside the barrier, which means that the electrons outside the barrier will transform into holes inside it, or vice versa. According to the boundary conditions, the corresponding transmission coefficient is

$$\mathscr{T}_{\rm b} = \left[1+\frac{\left(k_x^2+\beta^2\right)^2}{4k_x^2\beta^2}\sinh^2(\beta D)\right]^{-1}, \tag{10}$$

which is known to attenuate exponentially with the incident energy E decreasing, so that the potential barrier can be viewed as reflecting the massive Dirac fermions completely. The solid line in Fig. 1(a) shows the transmission of the electrons in the bilayer graphene when $\phi = 0$. It is illustrated that the normal incident massive Dirac fermions will be reflected completely when $E < U_0$ but can transmit perfectly at resonant conditions $q_xD = m\pi$ when $E > U_0$.

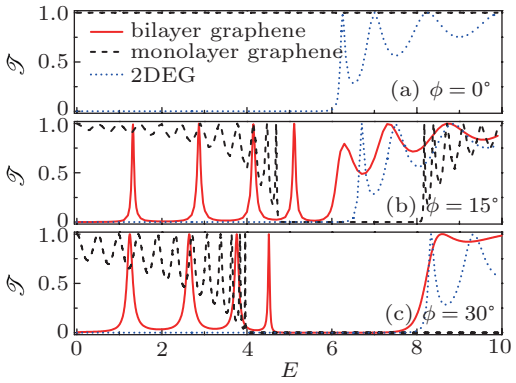


Fig. 1. (color online) Dependences of the transmission on the incident energy for the bilayer graphene, the monolayer graphene, and the 2DEG. The height and width of the potential barrier are $U_0 = 6$ and $D = 2\pi$, respectively, and (a) $\phi = 0°$, (b) $\phi = 15°$, and (c) $\phi = 30°$.

It is very interesting to find that the transmission with normal incidence in the bilayer graphene is identical to that in 2DEG, as the dotted line shows in Fig. 1(a), no matter for the low barrier or the high barrier. However, the transmission in the monolayer graphene is completely different, which reaches unity at $\phi = 0$ with arbitrary high barrier, and is called Klein tunneling.[6] It is elucidated that though the Dirac fermions in the bilayer graphene are described by spinor wavefunctions as those in the monolayer graphene, the transmission with normal incidence is the same as that of the unrelativistic electrons in the 2DEG. The result originates from the fact that the electrons in the bilayer graphene and the 2DEG are both massive and have a parabolic dispersion but those in the monolayer graphene are massless and possess a linear dispersion.

Second, for the non-normal incidence, it is generally known that the transmission in the 2DEG still oscillates for low barriers but decays exponentially for high barriers, and the expression of the transmission coefficient can be simplified to the form in Eqs. (9) and (10). In our previous work, it is found that in the monolayer graphene, the transmission has a gap with the edges $E = U_0/(1\pm\sin|\phi|)$ due to the evanescent mode inside the barrier.[29,30] However, the transmission in the bilayer graphene demonstrates a dramatic difference compared with that in the two materials above. There are resonant peaks for a high barrier, which exist in the transmission profile of the monolayer graphene but do not appear in that of the 2DEG. It indicates that the electrons outside the barrier at oblique incidence can transform into holes inside it (or vice versa) so as to transport through the barrier perfectly for both the monolayer graphene and the bilayer graphene, but can only be reflected at the interface of the barrier for the 2DEG, which originates from the gapless energy spectrum and the chiral nature of the quasiparticles in the two graphene systems.

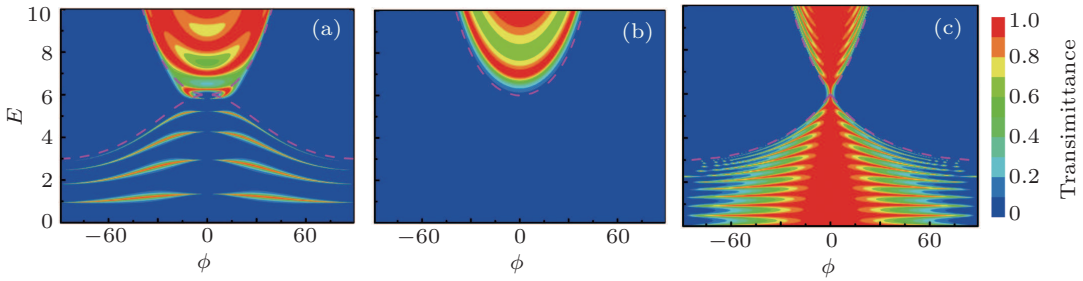


Fig. 2. (color online) Contour plots of the transmission through a potential barrier (with height $U_0 = 6$ and width $D = 2\pi$) for (a) the bilayer graphene, (b) the 2DEG, and (c) the monolayer graphene. The dashed lines in each figure imply the transport conditions, which are also the division of the tunneling and the forbidden regions.

Figure 2 further reveals the dependences of the transmission on the incident energy and the incident angle for the three materials. It is found that there are tunneling and forbidden regions in each figure, and they are divided by the dashed lines clearly. In fact, the dashed lines in the figure represent the transport conditions involving the incident energy and the incident angle, which satisfy $E = U_0/\left(1 \pm \sin^2\phi\right)$ for the bilayer graphene, $E = U_0/\left(1 \pm |\sin\phi|\right)$ for the monolayer graphene, and $E = U_0/\cos^2\phi$ for the 2DEG. When the incident energy or the incident angle is tuned outside the tunneling region, no electronic states will be contained inside the barrier, which makes the transmission coefficient attenuate exponentially and leads to the forbidden region in the transmission spectrum.

Owing to the pseudospins and the charities of the quasiparticles, the tunneling region covers from $E < U_0$ to $E > U_0$ for the two graphene systems, while it only exists when $E > U_0$ for the 2DEG. For the case of $E < U_0$, the electrons in the monolayer graphene can be tuned to transmit perfectly as like the barrier is transparent in many situations. However, those in the bilayer graphene can transport with a high transmission coefficient only when the incident energy and the incident angle satisfy strict conditions, which correspond to the narrow resonant regions in the lower part of Fig. 2(a). The resonant regions are so narrow that the transmission in the bilayer graphene through the high barrier may be used for a high-performance energy or wave filter.

For $E > U_0$, the shape of the tunneling region for the bilayer graphene is the same as that for the 2DEG but different from that for the monolayer graphene, which results from the parabolic energy spectrum of the former two materials and the linear energy spectrum of the latter. The transmissions for this case in the former two materials are still totally different: for the wide-angle incidence (still inside the tunneling region), the transmission coefficient is very high as the incident energy E increases in the bilayer graphene, while oscillates as a function of E in the 2DEG, which is also shown in Fig. 1(c).

Figure 3 presents the conductance verse the Fermi energy E for the three materials. It is apparent that the conductance profiles of the three materials have dramatic differences. For the monolayer graphene, there is a forbidden region near the Dirac point, that is the region of almost zero conductance corresponding to the transmission gap.[29,30] For the 2DEG, the conductance approaches zero for high barriers and increases as the Fermi energy increases for low barriers, which agrees with the forbidden region for $E < U_0$ and the tunneling region for $E > U_0$ in Fig. 2(b). As a comparison, when $E < U_0$, there are some sharp oscillations in the conductance for the bilayer graphene, which originate from the line-type resonant regions in the transmission spectrum. The oscillations are so sharp (especially the falling-edge) that they may be used as a high-performance sensor sensitive to the Fermi energy. When $E > U_0$, the conductance is similar to that for the 2DEG, just bigger than the latter, which agrees with the analysis about the transmission spectrum in Fig. 2, that is, the shapes of the two materials are identical but the transmission coefficient of the former is higher than that of the latter.

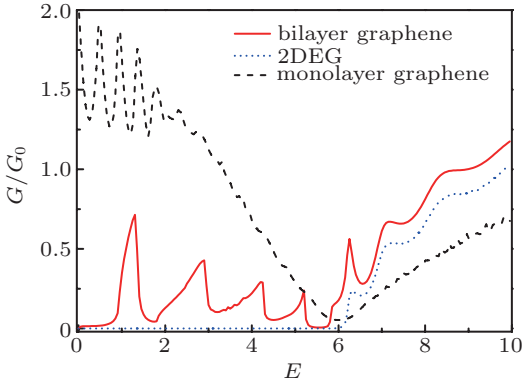


Fig. 3. (color online) Conductance as a function of the Fermi energy for bilayer graphene, monolayer graphene, and 2DEG. The height and width of the potential barrier are $U_0 = 6$ and $D = 2\pi$, respectively.

4. Conclusion

In summary, we investigated the transport properties of the electrons through a potential barrier in bilayer graphene and compared them with those in monolayer graphene and the conventional semiconductors (the 2DEG) to understand the nature of the massive Dirac fermions. It is found that the transmission with normal incidence in the bilayer graphene is identical to that in the 2DEG but totally different from that in the monolayer graphene for both high ($E < U_0$) and low

($E > U_0$) barriers. However, when the electrons in the bilayer graphene transport through the high barrier non-normally, resonant peaks appear, which exist in the transmission profile of the monolayer graphene but will not occur in that of the 2DEG. The transport properties elucidated above originate from the parabolic energy spectrum and the chiral nature of the massive Dirac fermions, respectively. There are tunneling and forbidden regions in the transmission spectra for the three materials, and the division of the two regions has been given in this work. For the two graphene systems, the tunneling region covers from $E < U_0$ to $E > U_0$, while it only exists when $E > U_0$ for the 2DEG. And in the $E > U_0$ case, the shape of the tunneling region for the bilayer graphene is the same as that for the 2DEG but different from that for the monolayer graphene. The counterpart of the resonant peaks through the high barrier is the sharp oscillations in the conductance profile of the bilayer graphene when $E > U_0$, which may be used as an excellent device sensitive to the Fermi energy.

References

[1] Beenakker C W 2008 *Rev. Mod. Phys.* **80** 1337
[2] Castro Neto A H, Guinea F, Peres N M R, Novoselov K S and Geim A K 2009 *Rev. Mod. Phys.* **81** 109
[3] Novoselov K S, Geim A K, Morozov S V, Jiang D, Zhang Y, Dubonos S V, Gregorieva I V and Firsov A A 2004 *Science* **306** 666
[4] Zhang Y, Tan Y W, Stormer H L and Kim P 2005 *Nature* **438** 201
[5] Zhang Y, Jiang Z, Small J P, Purewal M S, Tan Y W, Fazlollahi M, Chudow J D, Jaszczak J A, Stormer H L and Kim P 2006 *Phys. Rev. Lett.* **96** 136806
[6] Katsnelson M I, Novoselov K S and Geim A K 2006 *Nature Phys.* **2** 620
[7] Novoselov K S, Geim A K, Morozov S V, Jiang D, Katsnelson M I, Gregorieva I V, Dubonos S V and Firsov A A 2005 *Nature* **438** 197
[8] Gusynin V P and Sharapov S G 2005 *Phys. Rev. Lett.* **95** 146801
[9] McCann E and Falḱo V I 2006 *Phys. Rev. Lett.* **96** 086805
[10] Zheng Y and Ando T 2002 *Phys. Rev. B* **65** 245420
[11] Zhang Y, Small J P, Amori M E S and Kim P 2005 *Phys. Rev. Lett.* **94** 176803
[12] Novoselov K S, McCann E, Mozorov S V, Fal'ko V I, Katsnelson M I, Zeitler U, Jiang D, Schedin F and Geim A K 2006 *Nature Phys.* **2** 177
[13] Tworzydlo J, Trauzettel B, Titov M, Rycerz A and Beenakker C W J 2006 *Phys. Rev. Lett.* **96** 246802
[14] Katsnelson M I 2006 *Eur. Phys. J. B* **52** 151
[15] Hu S J, Du W, Zhang G P, Gao M, Lu Z Y and Wang X Q 2012 *Chin. Phys. Lett.* **29** 057201
[16] Beenakker C W J 2006 *Phys. Rev. Lett.* **97** 067007
[17] Bhattacharjee S and Sengupta K 2006 *Phys. Rev. Lett.* **97** 217001
[18] Bai C X and Zhang X D 2007 *Phys. Rev. B* **76** 075430
[19] McCann E 2006 *Phys. Rev. B* **74** 161403
[20] Ohta T, Bostwick A, Seyller T, Horn K and Rotenberg E 2006 *Science* **313** 951
[21] Oostinga J B, Heersche H B, Liu X, Morpurgo A and Vandersypen L M K 2008 *Nature Mater.* **7** 151
[22] Castro E V, Novoselov K S, Morozov S V, Peres N M R, Lopes dos Santos J, Nilsson J, Guinea F, Geim A K and Castro Neto A H 2007 *Phys. Rev. Lett.* **99** 216802
[23] San-Jose P, Prada E, McCann E and Schomerus H 2009 *Phys. Rev. Lett.* **102** 247204
[24] Nilsson J, Castro Neto A H, Guinea F and Peres N M R 2007 *Phys. Rev. B* **76** 165416
[25] Masir M R, Vasilopoulos P and Peeters F M 2009 *Phys. Rev. B* **79** 035409
[26] Park S H and Sim H S 2009 *Phys. Rev. Lett.* **103** 196802
[27] Mikitik G P and Sharlai Yu V 2008 *Phys. Rev. B* **77** 113407
[28] Mukhopadhyay S, Biswas R and Sinha C 2010 *Phys. Status Solidi B* **247** 342
[29] Chen X and Tao J W 2009 *Appl. Phys. Lett.* **94** 262102
[30] Sun L F and Guo Y 2011 *J. Appl. Phys.* **109** 123719
[31] Zhang G P and Qin Z J 2011 *Chem. Phys. Lett.* **516** 225